Drilling of K-60 Alumina Ceramic with Different Grades of Abrasives at Various Temperatures using Fluidized Bed-Hot Abrasive Jet Machining (FB-HAJM) Process

Subhadip Pradhan[1], Ranjit Kumar Behera[2], Basanta Kumar Nanda[3], Sudhansu Ranjan das[4] and Debabrata Dhupal[5]

[1,3]School of Mechanical Engineering, KIIT University, Bhubaneswar, India
[2, 4, 5] VSSUT, Burla

E-mail: basantananda_2005@yahoo.co.in

Abstract. This paper is focused on drilling of K-60 alumina ceramic using various grades of hot abrasives at different temperatures with pressurized and fluidized bed abrasive jet machining (FB-AJM) process. The fluidized bed mixing chamber, pressurized powder feed system, and abrasive heating chamber are fabricated and modified to study the effects of different machining parameters, like, pressure, standoff-distance, grain size, and temperature on material removal rate and taper angle. Box Behnken Design of Response Surface Methodology is used to study the parametric effect on responses. Finally, a single experiment is performed at the predicted optimal condition, obtained from the multi-response particle swarm optimization to validate the model.

***Keywords*:** FB-AJM, K-60 alumina ceramic, Response Surface Methodology, Desirability function, PSO.

1. Introduction

Abrasive Jet Machining (AJM) is an economic and efficient process to perform surface contouring, polishing, etching, machining, drilling, and deburring operations on hard and fragile materials like alumina ceramics, quartz, glass, semiconductor materials, super alloys, mica, and refractory materials. The repeated impingement of fine abrasive particles with high kinetic energy creates cracks on the target surface and removes the material. Then, the high velocity carrier gas removes the dislodge microscopic particles from the machined surface. The proper selection and utilization of the machining parameters make the AJM process efficient, economical and hassle free so that a large number of tedious, costly, and time consuming experimental observations can be reduced. Many researchers in the past explained about the influence of different process parameters affecting the responses like material removal rate, surface finish, depth of cut, side wall erosion, flaring, and etc. Some researchers have made the numerical analysis, experimental analysis along with different techniques of optimization, and necessary modifications in the different parts of the AJM process so as to increase its effectiveness.

Balasubramaniam et al. [1][2] generated the shape of the machined surface by AJM and analyzed the effects of various input parameters such as abrasive grit size, mixing ratio, nozzle diameter, stand-off-distance and the thickness of the specimen on the output parameters by using the Taguchi orthogonal array design for plaster-of-paris and AISI 304 stainless steel burr specimens. Jafar et al. [3][4] applied the technique of abrasive jet micro-machining (AJMM) to erode features like micro-electro-mechanical and micro-fluidic device for fabrications of unmasked channels in borosilicate glass and experimentally analyzed the effect of particle size, velocity, and angle of attack in AJM. Sooraj et al. [5] proposed the novel approach of using elastic abrasives for the purpose of inner surfaces of tubular specimens and used one mathematical model for the mechanism of material removal rate (MRR).Implementation of the high erosion resistant, thick mask of SU-8 layer during fabricating of 3-D micro-channel on a glass slide was also performed [6] . Generation of the uniform erosive flux was carried out by Ghobeity et al. [7][8] for flat masked and unmasked planar areas of constant elevation for machining the oscillating target material with respect to the nozzle and described the analytical models for the uniformity of the particles. Liu et al. [9] investigated the abrasive enhanced electrochemical slurry-jet-machining (ESJM) of metals using both abrasive slurry-jet machining and electrochemical jet machining to conclude that roughness varied inversely with the erosion rate. Burzynski and Papini [10] successfully performed the surface evolution of the glass workpieces by using the narrow band level set methodology. The erosion rate of poly-methyl-methacrylate (PMMA) was conducted by Getu et al. [11] using Al_2O_3 particles, and analyzed the experimental results to propose the novel models. Hadevi et al. [12] obtained the influence of pressure on particle orientation at a given nozzle-tip-distance (NTD) by modeling of instantaneous particle orientation and it was correlated with the embedding virgin surfaces. Preparation of the cutting edge micro-shape, sensitivity and reproducibility of wet abrasive jet machining were evaluated [13] to obtain that air jet feed, speed and relative jet inclination angle had a strong impact on the cutting edge and form factor. The various machining properties such as material removal rate (MRR), surface roughness (Ra), and etc. were optimized in the past by applying different optimization techniques for the effective utilization of the machining parameters. Zhang et al. [14] applied Taguchi orthogonal array and multi-variable linear regression method to the micro abrasive intermittent jet machining (MAIJM) process where no abrasive was injected into the gas stream for a period of time and the continuous flow of gas without abrasives took off the accumulated particles in the hole. The multi-response optimization of machining parameters of glass work-pieces in AJM was successfully performed by Routara et al. [15] with the help of Taguchi orthogonal array and grey relational analysis. The novel concept of genetic approach and fuzzy logic were investigated by Chakravarthy et al. [16] for the purpose of abrasive water jet cutting of paradise granite. Fluidised bed abrasive jet machining (FB-AJM) is an effective development of the AJM process to produce a homogeneous mixture of abrasives and air so that better machined surface can be obtained. Barletta et al. [17] proposed the fluidized bed abrasive jet machining (FB-AJM) system for finishing the internal part of narrow and long tubular components of stainless steel and high strength ductile aluminium alloy (AA 6082 T6). Nanda et al. [18][19] proposed the Box-Behnken response surface methodology for conducting the FB-AJM experiments on K-99 alumina ceramic and GFRP materials using different grades of SiC abrasives and applied the particle swarm optimization (PSO) technique to obtain the optimal conditions of input factors. Jagannatha et al. [20][21] used the noble concept of hot air as carrier media in AJM to carry out experiment on glass etching and grooving by using abrasive hot air jet machining (AHAJM) and studied the effect of air temperature on material removal rate and surface roughness applied to the process of glass etching and grooving to get the optimal conditions of input parameters.

Alumina ceramic (K-60) is a versatile material for use in domestic applications but difficulties arise in its machining operation with proper accuracy. In this novel approach, abrasive particles are heated for the purpose of producing sharp edges so as to increase the process precision and to decrease the embedment of abrasive particles on to the work-piece. This paper is focused on hot abrasive fluidized bed abrasive jet machining (HA-FBAJM) of hard and brittle alumina ceramic (K-60) materials using hot SiC abrasive at different temperatures with the FB-AJM set up based on pressurized powder feed and fluidized mixing chamber. The influence of four machining parameters viz. pressure (P), stand-off

distance (S), Temperature (T), and abrasive size (G) on the responses like material removal rate (MRR) and taper angle (TA) are experimentally analyzed according to Box-Behnken Design of response surface methodology. Then regression models are developed, desirability functions are defined, and then Particle Swarm Optimization (PSO) technique is applied. Finally, these results are experimentally validated.

2. Experimental Details

2.1 Experimental procedure

The fluidized bed-hot abrasive jet machining (FB-HAJM) is shown in Fig.1and Fig.2, which consists of a mixing chamber, heating chamber, nozzle, thermocouple, regulator, compressor, and other accessories. The heating chamber consists of a heating coil of 1500 watts, which is controlled by a voltage regulator so that the required temperature of heating can be achieved. It is mounted inside the funnel type chamber and connected to the thermocouple for the accurate temperature required for the experimentation. The end part of the heating chamber is connected to a flow control device for smooth flow into the mixing chamber. A multi-stage air compressor of 5 kW power with 12 bars of the working pressure is used to supply high pressure air as the carrier medium. The compressed air is then passed through the Filter-Regulator-Lubricator (FRL) or dehumidifier to produce clean and dry air so that abrasives can flow through the nozzle without clogging. The high carbon and high chromium D2 steel material is used to manufacture the nozzle due to its high abrasion resistance property. The experiments are conducted in the airtight machining chamber to prevent the leakage of fine abrasive particles to the surrounding. After filtration, the compressed air passes through a regulator and enters into the mixing chamber. The abrasive particles of proper grain size with required amount are heated in the heating chamber. Then the stop valve is opened manually after the required temperature is reached and allowing the hot abrasives to enter into the mixing chamber to mix with the high pressurized air. The fluidized bed makes the upward flow of the high speed air from the bottom of the reservoir through these abrasives to produce a uniform and homogeneous air-hot abrasive mixture, and creates a cloud of suspended particles at the nozzle inlet.

Figure 1.FB-HAJM System

Figure 2. Heating chamber with Thermocouple

2.2 Specification of abrasive materials

Silicon carbide (SiC) abrasives with three different sizes of 745µm, 525µm and 185µm are used for this experiment. The details of the chemical composition, 3 grades of abrasives and one microstructure are given below.

Al_2O_3 99.8% ,	SiO_2 0.03% ,	Fe_2O 0.02%	Na_2O 0.07%.	MgO 0.05%.	and CaO 0.02%

Figure 3. Silicon-carbide (SiC) abrasives of 3 different grit size

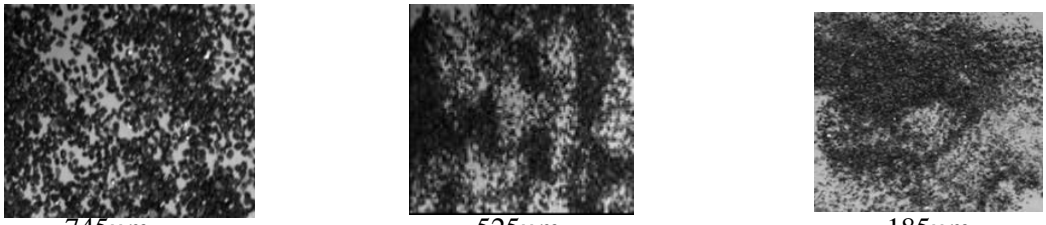

Figure 4. SEM micrograph of silicon-carbide (SiC) abrasives

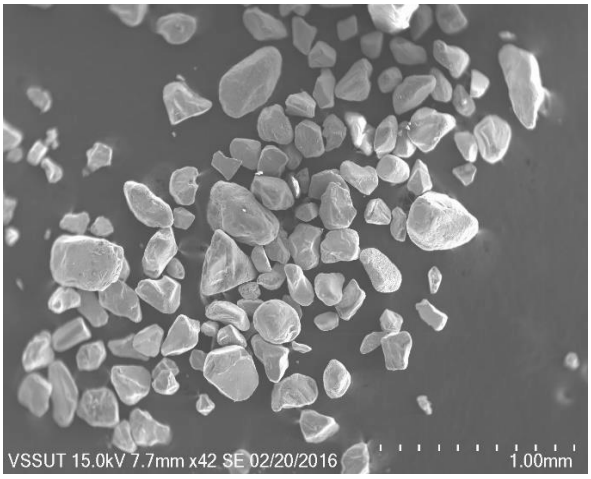

2.3 Details of work piece materials

K-60 alumina ceramic plates of dimension 25mm x 25mm x5mm are used as the work-piece materials for this experimental purposes. The figure of some machined work piece and one of its SEM figure is shown below.

Figure 5. Machined alumina ceramics workpiece materials

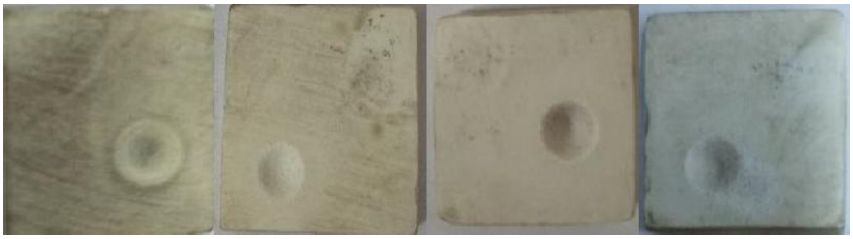

Figure 6. SEM micrograph of machined workpiece

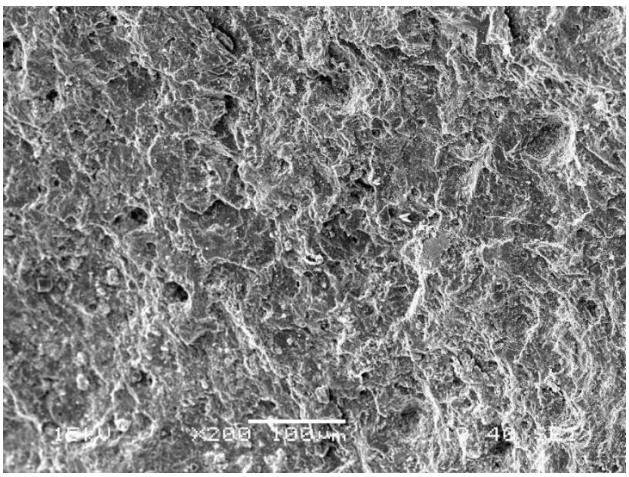

2.4 Input process parameters and responses

Proper selection of the input machining parameters with their levels are important to achieve the best output results. Here, pressure (P), temperature (T), standoff distance(S) and grain size (G) are taken to measure the different outputs such as the material removal rate (MRR) and taper angle (TA).

The following responses are measured for this experimentation.

2.4.1 Measurement of Material removal rate (MRR)

Material removal rate (w) is calculated on mass (g/s) basis as $W = \frac{(W_1 - W_2)}{\Delta t}$,

Where, W_1 and W_2 (gm.) are the weights of the specimen before and after machining for a time span of Δt. The weights are measured by a digital weighing machine ol LC 0.001gram.

2.4.2 Measurement of taper angle (TA)

The drilled-hole in AJM resembles a truncated cone in which the tapered angles are generated on the surface as shown in Fig.5,and it is measured with the use of formula, Taper angle, $TA = tan^{-1}\left[\frac{D_1 - D_2}{2h}\right]$,

where, D_1 = Outer diameter of machined work-piece,

D_2= Inner diameter of machined work-piece, and

h = Depth of cut.

The above dimensions are accurately measured with the help of Co-ordinate measuring machine (CMM, 876, Zeiss MC850 with stylus and a probe attachment).as shown in Fig.8.

Figure 7: Tapper angle (T_A)

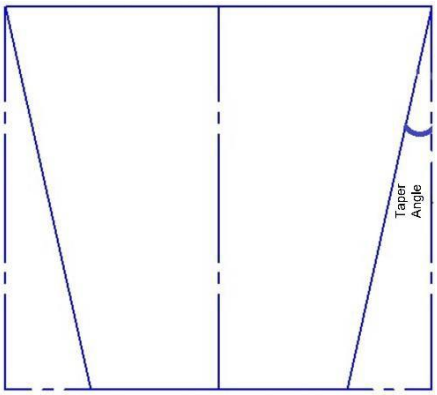

Figure 8: Co-ordinate Measuring Machine

3. Design of Experiment

Design of experiment (DOE) explains about the conduct of the experiment and analysis of data. Here, experiments are performed according to Box-Behnken design (BBD) of response surface methodology (RSM) with four input parameters i.e. pressure (P), stand-off distance (S), grain size (G), and temperature (T), each with three levels i.e. low (-1), mid (0) and high (+1) for obtaining 15 number of observations to measure MRR (W) and taper angle (TA).Generally, RSM is used to analyze problems with several variables influencing the response and the purpose is to optimize the response Y with model $Y = f(X_1, X_2)$, where $f(X_1, X_2)$ is the response surface. The contours of the response surface indicate the line of constant response. RSM is exclusively used to examine the "surface," which is the relationship between the response and the factors affecting the response. The method of steepest ascent represents maximization and the method of steepest descent represents the minimization of the response. The exact nature of the response is unknown and the model is an attempt to approximate it. The objective is to optimize a response which is influenced by several independent input variables by a careful design of experiments. The fitted model is used to arrive at the best operating conditions that result in either a maximum or minimum response. If more number of responses are to be optimized simultaneously, then desirability functions are useful in that case. All the statistical calculations and surface plots and are performed with Design Expert software. The input parameters with their three different levels are shown in Table 1.

Table 1. Experimentational Analysis

Sl. No.	Input Parameters				Output Parameters	
	P (bar)	T(°C)	SOD(mm)	GS(µm)	MRR	TA
1	3	80	8	525	0.001093	69.7956
2	7	80	6	745	0.005042	40.26004
3	5	80	6	525	0.003568	30.13002
4	7	80	8	525	0.004982	38.65226
5	3	80	6	185	0.002557	54.61844
6	5	100	4	525	0.00244	31.46027
7	3	100	6	525	0.002715	3.268356
8	5	80	6	525	0.003928	35.8095
9	7	60	6	525	0.004048	4.852828
10	5	80	8	185	0.00633	35.88153

11	5	80	4	185	0.001142	53.53394
12	7	100	6	525	0.006206	35.9597
13	5	80	4	745	0.003277	41.66128
14	5	80	6	525	0.002782	49.23998
15	3	60	6	525	0.002271	61.15482
16	5	100	8	525	0.00788	41.12401
17	5	80	8	745	0.00604	44.11692
18	5	60	4	525	0.001071	54.52504
19	3	80	4	525	0.00222	48.83972
20	5	100	6	745	0.00545	30.19024
21	7	80	6	185	0.00445	26.866
22	5	60	6	185	0.004031	30.67902
23	7	80	4	525	0.0044	27.97186
24	3	80	6	745	0.002493	56.11001
25	5	60	6	745	0.00406	42.54281
26	5	60	8	525	0.004784	16.06724
27	5	100	6	185	0.00384	36.05405

4. Experimental results and discussions

The results obtained for the K-60 alumina ceramic material (as shown in Table 1) are put in the Design Expert software to find the most significant variable, p-values, Lack of Fit Values, R^2 and Adj- R^2-values of the response models from the Analysis of Variance (ANOVA) as shown in Table 2. The various surface plots have been developed as the result of this experimentation which are very important for analysis of input process parameters.

4.1 Adequacy test of responses

The data obtained from the measurements are put in the Design Expert software and the analysis of variance (ANOVA) is obtained to find the most significant variables affecting the responses i.e. material removal rate (MRR) and taper angle (TA). Regression analysis is also performed for each of the responses and the following quadratic models are developed as given in equation. 1, and 2.

$$MRR = .015079 - 3.44849*10^{-4} * P - 3.33330*10^{-4} * T - 4.43542*10^{-4} * S - 6.79592*10^{-6} * G + 1.07125*10^{-5} * P * T + 1.06813*10^{-4} * P * S + 3.60056*10^{-7} * P * G + 1.07937*10^{-5} * T * S + 8.29301*10^{-8} * T * G - 1.27611*10^{-6} * S * G - 6.77396*10^{-5} * P^2 + 1.29729*10^{-6} * T^2 + 3.16979*10^{-5} * S^2 + 7.75481*10^{-9} * G^2 \quad (1)$$

$$TA = 346.83312 - 50.28578* P - 0.59209* T - 41.78053* S - 0.067540* G + 0.55621* P * T - 0.64222* P * S + 5.51416*10^{-3} * P * G + 3.0076 * T * S - 8.01420*10^{-4} * T * G + 9.73851*10^{-3} * S* G + 0.18901* P^2 - 0.023257* T^2 + 1.29151* S^2 + 5.46073*10^{-5} * G^2 \quad (2)$$

Table 2 ANOVA Table for MRR and TA

Response	p-value	Lack of Fit	R-squared	Adj R-squared
MRR	0.0242	4.42	0.9329	0.8122
TA	0.0464	0.3980	0.7587	0.4772

4.2 Analysis of surface plot

From the surface plot of MRR vs. Temperature and Pressure, it is seen that MRR increases with increase of pressure but the rate of increase is slower at higher pressure MRR first decreases slowly with increase in pressure and after that it increases gradually. From the surface plot of MRR vs. Pressure and Grain size, it is seen that MRR initially decreases with increase in grain size and after that it increases due to high in Fig. 9.

Figure 9. Surface Plot of MRR vs P and T

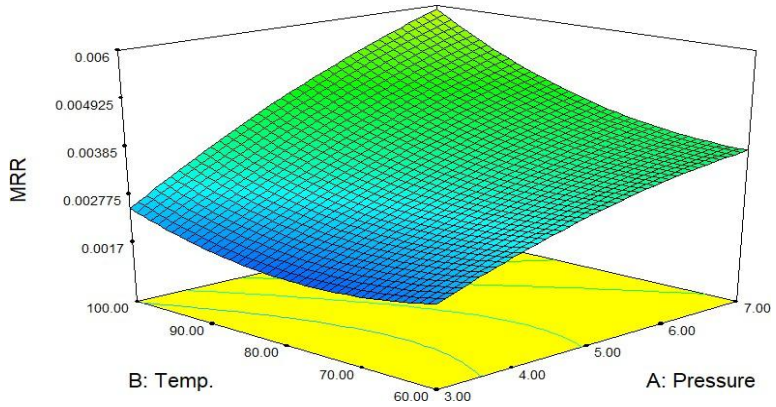

From the surface plot of taper angle (TA) it is seen that TA decreases with increase in pressure, first increases and then decreases with respect to temperature, and also SOD. One such surface plot graph is given in Fig.10**.**

Figure 10. Plot of TA vs. Grain size and SOD

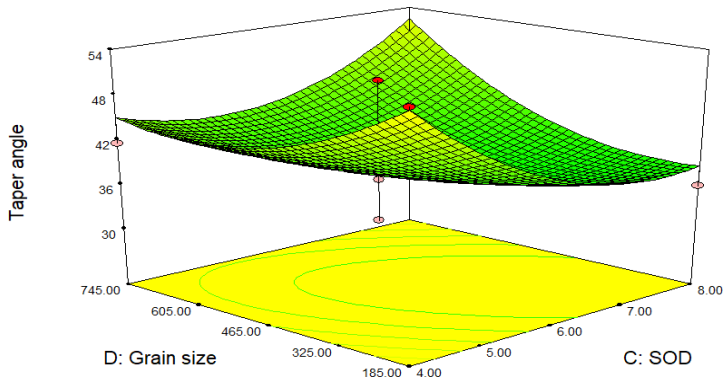

5. Desirability based Particle Swarm Optimization (PSO)

5.1 Desirability Function

Desirability based multi-objective optimization was performed on the concept of Derringer and Suich, in which each and every output is converted into a global desirability function as given in equation (3)

where, U_i =Upper, L_i = lower, and T_i = Target values of each output with powers "s" and "t" as the weights (w_j) set by the experimenter By combining all these individual desirability indices, the global desirability index (D) is determined as per equation (4) with n = total number of objectives, and w_j = individual weights, in a scale from 1 to 5 (1 for the least and 5 for the highest importance). The weight distribution and Desirability Function of the objectives are shown in Table 3.

$$d_i(\hat{y}_i(x)) = \begin{cases} 0 & if \quad \hat{y}_i(x) < L_i \\ \left(\dfrac{\hat{y}_i(x) - L_i}{T_i - L_i}\right)^s & if \quad L_i \le \hat{y}_i(x) < T_i \\ 1 & if \quad \hat{y}_i(x) = T_i \\ \left(\dfrac{\hat{y}_i(x) - U_i}{T_i - U_i}\right)^t & if \quad T_i \le \hat{y}_i(x) \le U \\ 0 & if \quad \hat{y}_i(x) > U_i \end{cases} \tag{3}$$

And desirability index, $D = (d^{r1}_1 \times d^{r2}_2 \times \ldots \times d^{rn}_n)^{1/\Sigma w_j}$ (4)

The Global Desirability Function (DF_i) and Fitness Function Y are defined as:

$$D = \left(d_1^{r_1} \times d_2^{r_2}\right)^{1/\Sigma w_J} \tag{5}$$

And $Y = \dfrac{1}{1 + DF}$ (6)

Table 3 Assigned weights to responses

Sl.No	Output	Optimization Objective	Desirability Function (Di)	Weight (w_i)
1	MRR	Maximum	$D_1 = \dfrac{MRR - MRR_{min}}{MRR_{max} - MRR_{min}}$	5
2	TA	Minimum	$D_2 = \dfrac{TA_{max} - TA}{TA_{max} - TA_{min}}$	5

5.2 Implementation of PSO

The designed particle swarm optimization (PSO) problem is presented as:
Minimize Y, subjected to Xmin.≤ X ≤ Xmax
where, Y is objective function , X stands for input parameter as X={P,Z,G,T},within the following ranges: 3 ≤ P ≤ 7, 4 ≤ S ≤ 8, 185 ≤ G ≤ 745, and 60 ≤ T ≤ 100
An initial swarm size of 50, number of iterations 200 with constants C_1 and C_2 as 2 are put in the PSO code, and made to run in MATLAB to obtain the predicted output as given in Table 4.

Table 4 PSO of input process parameters and responses

Type of Model	Process Parameters				Response values	
	P	SOD	GS	T	MRR	TA
Predicted	5	6	525	80	0.004396	36.799
Actual Experiment	5	6	525	80	0.003928	35.8095
Error %	---				10.646%	2.76%

The predicted optimal values are validated experimentally to find the % of errors as shown in Table 5. Due to less % of deviation between the actual experimental value and predicted values, the PSO of the FB-AJM conditions is validated.

6. Conclusion

The following outcomes can be drawn from the above experimental analysis which is a development of the recent advances in AJM process:

1. Better material removal rate (MRR) is achieved at parametric combinations of high pressure, mid-value of stand-off distance, higher grain sizes, and mid values of Temperature. Taper angle is less at high pressure, nozzle tip distance, mid-value of grain sizes, and lower values of temperature.
2. The predicted optimal combination of parameter setting are pressure of 7 kgf/cm^2, stand-off distance of 8 mm , grain size of 745µm and temperature of 80°C for achieving the optimal output, i.e. MRR of 0.005413g/s, and taper angle of 40.801262.
3. Experiment is performed at predicted optimal conditions to validate the optimality of the model and the measured experimental responses values obtained are MRR of 0.004982gm/s, and taper angle of 38.65226 degree. The percentage of errors between the predicted models and experimental values are less and within the specified range
4. The present research work of AJM on rectangular work piece of borosilicate glass material will be useful for the modern engineering industries those are working in the field of machining and fabrication of glass, ceramic and other precious brittle materials.

References

[1] Balasubramaniam R, Krishnan J and Ramakrishnan N 2002 A study on the shape of the surface generated by abrasive jet machining *J. Mater. Process. Technol.* **121** 102–6
[2] Balasubramaniam R, Krishnan J and Ramakrishnan N 1999 Experimental study on the abrasive jet deburring of cross-drilled holes *J. Mater. Process. Technol.* **91** 178–82
[3] Jafar R H M, Hadavi V, Spelt J K and Papini M 2016 Dust reduction in abrasive jet micro-machining using liquid films *Powder Technol.* **301** 1270–4
[4] Mohammad Jafar R H, Spelt J K and Papini M 2013 Numerical simulation of surface roughness and erosion rate of abrasive jet micro-machined channels *Wear* **303** 302–12
[5] Sooraj V S and Radhakrishnan V 2014 Fine finishing of internal surfaces using elastic abrasives *Int. J. Mach. Tools Manuf.* **78** 30–40
[6] Saragih A S and Ko T J 2009 A thick SU-8 mask for microabrasive jet machining on glass *Int. J. Adv. Manuf. Technol.* **41** 734–40
[7] Ghobeity A, Papini M and Spelt J K 2009 Abrasive jet micro-machining of planar areas and transitional slopes in glass using target oscillation *J. Mater. Process. Technol.* **209** 5123–32
[8] Ghobeity A, Ciampini D and Papini M 2009 An analytical model of the effect of particle size distribution on the surface profile evolution in abrasive jet micromachining *J. Mater. Process.*

Technol. **209** 6067–77
[9] Liu Z, Nouraei H, Papini M and Spelt J K 2014 Abrasive enhanced electrochemical slurry jet micro-machining: Comparative experiments and synergistic effects *J. Mater. Process. Technol.* **214** 1886–94
[10] Burzynski T and Papini M 2011 A level set methodology for predicting the surface evolution of inclined masked micro-channels resulting from abrasive jet micro-machining at oblique incidence *Int. J. Mach. Tools Manuf.* **51** 628–41
[11] Getu H, Ghobeity A, Spelt J K and Papini M 2007 Abrasive jet micromachining of polymethylmethacrylate *Wear* **263** 1008–15
[12] Hadavi V, Michaelsen B and Papini M 2015 Measurements and modeling of instantaneous particle orientation within abrasive air jets and implications for particle embedding *Wear* **336–337** 9–20
[13] Biermann D, Aßmuth R, Schumann S, Rieger M and Kuhlenkötter B 2016 Wet Abrasive Jet Machining to Prepare and Design the Cutting Edge Micro Shape *Procedia CIRP* **45** 195–8
[14] Zhang L, Kuriyagawa T, Yasutomi Y and Zhao J 2005 Investigation into micro abrasive intermittent jet machining *Int. J. Mach. Tools Manuf.* **45** 873–9
[15] Thatoi D N and Nayak B B 2011 Optimisation of multiple performance characteristics in abrasive jet machining using grey relational analysis Bharat Chandra Routara *, B . K . Nanda and Ashok Kumar Sahoo *Technology* **24** 4–22
[16] Sitarama Chakravarthy P and Ramesh Babu N 1999 A New Approach for Selection of Optimal Process Parameters in Abrasive Water Jet Cutting *Mater. Manuf. Process.* **14** 581–600
[17] Barletta M, Rubino G, Guarino S, Bolelli G, Lusvarghi L and Gisario A 2008 Fast Regime-Fluidized Bed Machining (FR-FBM) of Atmospheric Plasma Spraying (APS) TiO2 coatings *Surf. Coatings Technol.* **203** 855–61
[18] Nanda B K, Mishra A and Dhupal D 2017 Fluidized bed abrasive jet machining (FB-AJM) of K-99 alumina ceramic using SiC abrasives *Int. J. Adv. Manuf. Technol.* **90** 3655–72
[19] Nanda B K, Mishra A and Dhupal D 2016 Drilling of GFRP Flat Plates with Modified AJM Process using SiC Abrasives 0–5
[20] Jagannatha N, Somashekhar S H, Sadashivappa K and Arun K V. 2012 Machining of soda lime glass using abrasive hot air jet: An experimental study *Mach. Sci. Technol.* **16** 459–72
[21] Jagannatha N, Hiremath S S and Sadashivappa K 2012 Analysis and Parametric Optimization of Abrasive Hot Air Jet Machining for Glass Using Taguchi Method and Utility Concept **7** 9–15